

Laser spectroscopy of ${}^7,{}^{10}\text{Be}^+$ in an online ion trap

T. Nakamura,^{1,*} M. Wada,^{1,†} K. Okada,² A. Takamine,^{1,3} Y. Ishida,¹ Y. Yamazaki,^{1,3} T. Kambara,¹ Y. Kanai,¹ T. M. Kojima,¹ Y. Nakai,¹ N. Oshima,^{1,‡} A. Yoshida,⁴ T. Kubo,⁴ S. Ohtani,⁵ K. Noda,⁶ I. Katayama,⁷ V. Lioubimov,⁸ H. Wollnik,⁹ V. Varentsov,¹⁰ and H. A. Schuessler⁸

¹Atomic Physics Laboratory, RIKEN, 2-1 Hirosawa, Wako, Saitama 351-0198, Japan

²Department of Physics, Sophia University, Chiyoda, Tokyo 102-8554, Japan

³Graduate School of Arts and Science, The University of Tokyo, Meguro, Tokyo 153-8902, Japan

⁴Nishina Center for Accelerator Based Science, RIKEN, 2-1 Hirosawa, Wako, Saitama 351-0198, Japan

⁵Institute for Laser Science, The University of Electro-Communications, Chofu, Tokyo 182-8585, Japan

⁶Institute of Radiological Science, Inage, Chiba 263-8555, Japan

⁷Institute of Particle and Nuclear Studies, High Energy Accelerator Research Organization (KEK), Tsukuba, Ibaraki 305-0801, Japan

⁸Department of Physics, Texas A&M University, College Station, Texas 77843, USA

⁹II. Physikalisches Institut, Justus-Liebig-Universität Giessen, Heinrich-Buff-Ring 16, 35392, Giessen, Germany

¹⁰Kholopin Radium Institute, Saint Petersburg, Russia

(Received 29 August 2006; published 15 November 2006)

Radioactive beryllium isotope ions (${}^7\text{Be}^+$ and ${}^{10}\text{Be}^+$) that are provided by a projectile fragment separator with ≈ 1 GeV beams, as well as stable isotope ions (${}^9\text{Be}^+$) are stored and laser cooled in an online ion trap. Their absolute transition energies of the $2s\ ^2S_{1/2} \rightarrow 2p\ ^2P_{3/2}$ transition were measured with an accuracy of $\sim 10^{-8}$. In this way isotope shifts of beryllium ions were obtained and the differential mass polarization parameter $\kappa = -0.286\ 41(70)$ a.u. as well as the $2s\ ^2S \rightarrow 2p\ ^2P$ transition energy of an infinitely heavy beryllium ion $h\nu^\infty = 0.145\ 524\ 290(42)$ a.u. were determined for the first time.

DOI: [10.1103/PhysRevA.74.052503](https://doi.org/10.1103/PhysRevA.74.052503)

PACS number(s): 32.10.Bi, 32.10.Fn, 32.30.-r

I. INTRODUCTION

An online ion trap for nuclear laser spectroscopy has been developed at the prototype slow radioactive ion-beam facility (SLOWRI) of RIKEN. Energetic radioactive ion beams from a projectile fragment separator are decelerated and cooled in a gas catcher cell and the thermal ions are extracted and collected in a linear rf trap by a combination of dc and inhomogeneous rf fields (rf ion guide) [1–3]. This online ion trap is a generally applicable device and can now be used for various high-precision laser spectroscopies of stored radioactive ions, such as hyperfine structure spectroscopy of the beryllium isotopes [4,5] to determine the anomalous radius of the valence neutron of the neutron halo nucleus ${}^{11}\text{Be}$ [6], and to determine the charge radii of these beryllium isotopes through laser-laser double-resonance spectroscopy of laser-cooled ions.

Laser cooling is an essential prerequisite for these planned experiments. However, the exact resonant frequencies of the cooling transitions for radioactive beryllium isotopes are not known. In such light elements, the isotope shifts in the atomic transitions are larger than 10 GHz and their dominant parts are due to complicated multielectron correlations. Some theoretical works on the isotope shifts of the beryllium ion exist, however, the values contradict each other. We worked and report on the measurements of these resonant frequencies of ${}^7\text{Be}^+$ and ${}^{10}\text{Be}^+$ in the online ion trap.

The Hamiltonian H_M for an N -electron atomic system with a nuclear mass M_n can be written with a zeroth-order Hamiltonian H_∞ for an infinite nuclear mass and point nuclear charge as

$$H_M = \frac{\mu}{m_e} \left(H_\infty + \frac{1}{M_n} \sum_{i<j}^N \mathbf{p}_i \cdot \mathbf{p}_j \right),$$

where m_e is the electron mass; $\mu = M_n m_e / (M_n + m_e)$ the reduced electron mass, and \mathbf{p}_k is the momentum of the k th electron. The solution is obtained by the perturbation to H_∞ of the second term in parentheses, the electron correlation term, as

$$\epsilon(M_n) = \frac{\mu}{m_e} \left(\epsilon^\infty + \frac{1}{M_n} \left\langle \sum_{i<j}^N \mathbf{p}_i \cdot \mathbf{p}_j \right\rangle \right) = \epsilon^\infty - \frac{\mu}{M_n} \epsilon^\infty + \frac{\mu}{M_n} K,$$

where ϵ^∞ represents the energy levels of the atom with infinite mass and $K = \langle \sum_{i<j}^N \mathbf{p}_i \cdot \mathbf{p}_j \rangle / m_e$ is the mass polarization parameter. The second term is the so-called normal mass shift (NMS) and the third term is the specific mass shift (SMS). In reality, the finite volume of the nucleus causes another shift, the so-called field shift (FS). However, the magnitude of the FS in the cooling transition for the beryllium isotopes was evaluated to be less than 100 MHz and the differences among isotopes are less than 10 MHz, which is smaller than the uncertainty of the present experimental results. Therefore we have neglected the FS throughout the paper.

In the experiments, only the energy difference between the two energy levels (a, b) of a particular isotope is observed. The observable transition frequency ν_{obs} is

*t-nkmr@riken.jp

†mw@riken.jp

‡Present address: National Institute of Advanced Industrial Science and Technology (AIST), Tsukuba, Ibaraki 305-8568, Japan.

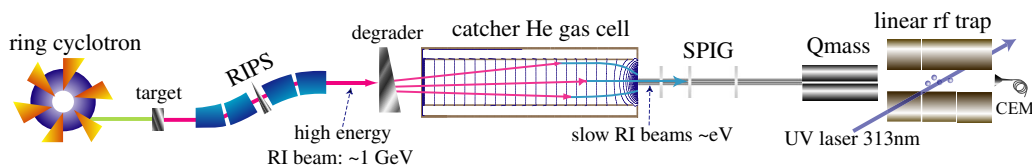


FIG. 1. (Color online) Schematic overview of the experimental apparatus.

$$h\nu_{\text{obs}} = \epsilon_a - \epsilon_b = h\nu^\infty - \frac{\mu}{M_n} h\nu^\infty + \frac{\mu}{M_n} \kappa, \quad (1)$$

where $\kappa = K_a - K_b$ is the differential mass polarization parameter and ν^∞ is the transition frequency of an infinitely heavy mass ion. Thus, one can experimentally determine ν^∞ and κ by measuring the resonance frequency of a particular transition for more than two isotopes. Since there is only one stable isotope in the beryllium element, the measurements on different radioactive isotopes are essential for this study.

II. EXPERIMENT

The experiments were carried out at the RIKEN projectile fragment separator facility, RIPS [7], where a prototype SLOWRI setup, which consists of a 2-m-long gas catcher cell with an rf carpet, a 60-cm-long SPIG (rf sixpole ion-beam guide) [8,9] and a linear rf trap are located downstream of RIPS (Fig. 1). A 100A-MeV ^{13}C beam from the RIKEN ring cyclotron hits a production target made of 10-mm-thick beryllium metal. The radioactive beryllium nuclei produced in the fragmentation reactions are mass separated by the RIPS. The energetic beryllium ions thus obtained are injected through an energy degrader into a gas catcher cell filled with 13 hPa He gas. The beryllium ions are thermalized in the gas cell and extracted by a combination of dc and inhomogeneous rf fields produced in the rf carpet. The extracted ions are sent to a linear rf trap located in an ultrahigh vacuum chamber through the SPIG. The impurity ions that are mainly produced in the gas cell are eliminated by a quadrupole mass filter. The linear rf trap used for spectroscopy is made of gold-plated aluminum blocks with a hyperbolic shape having an inner separation distance $2r_0$ of 16 mm. The electrodes are segmented into three 41-mm-long sections to provide an axial confinement field, and they are attached to a cryogenic head to reduce any impurities in the trap as well as to cool the buffer gas. The equilibrium temperature of the electrodes is estimated to be <50 K.

The moderated beryllium ions form a continuous beam of a few eV and are injected into the trap while pulsed He buffer gas is used at a pressure of 10 mPa. During the accumulation period, rf voltages of $\approx 400 V_{\text{pp}}$ at a frequency of 3.6 MHz are applied to the trap electrodes. However, in contrast, during the cooling period, the voltages are decreased to $\approx 100 V_{\text{pp}}$ to reduce rf heating effects on the trapped ions. Cw laser radiation of 313 nm is introduced to the center of the trap under an angle of 10° . This radiation is generated by a ring dye laser followed by second harmonic generation with an external cavity. The typical intensity of the radiation was 1 mW. Fluorescence photons are detected by a photo-

multiplier and a two-dimensional photon counter. The polarization of the radiation is controlled by rotating a $\lambda/4$ plate. A weak magnetic field of 0.54 mT is applied by a set of Helmholtz coils oriented along the direction of the laser radiation in order to define the quantization axis.

In our first online experiment, $^{10}\text{Be}^+$ ions were trapped and laser cooled down to well below 1 K. This meant that we achieved a 10^{13} -fold reduction in the kinetic energy of the ions, which was initially ≈ 1 GeV and finally cooled to ≈ 0.1 meV. However, since the asymmetric fluorescence profile of the laser-cooled ions is not adequate to accurately determine the resonant frequency of interest, we measured the spectra of buffer gas-cooled ions in the online experiments. Buffer gas-cooled spectra of $^7\text{Be}^+$ and $^{10}\text{Be}^+$ ions are shown in Fig. 2. Doppler-limited as well as Doppler-free saturated absorption signals of the 626 nm fundamental dye-laser radiation were simultaneously measured in a molecular iodine cell with the laser scan in order to calibrate with the absolute frequencies that are described in the spectral atlas of the iodine molecule [10]. The fringes of a 300-mm-long Fabry-Pérot étalon were also recorded to determine the scale of the scanning frequency. From these spectra, the peak frequencies of the buffer gas-cooled $^{7,10}\text{Be}^+$ ions, $\nu_{\text{gc}}^{7,10}$ were obtained to be

$$\nu_{\text{gc}}^7 = 957\,347.369(56) \text{ GHz} \quad \text{and}$$

$$\nu_{\text{gc}}^{10} = 957\,413.839(35) \text{ GHz}.$$

Since the Doppler width of these buffer gas-cooled spectra were larger than the possible width due to the hyperfine splittings, one can in general assume that the peak frequencies of the spectra reflect the transition between the centers of gravity of the hyperfine states. However, one must consider the possibility to have an asymmetric peak shape due to partial optical pumping even in such buffer gas-cooled spectra. We therefore experimentally verified this assumption with stable $^9\text{Be}^+$ ions by comparing buffer gas-cooled spectra with a narrow laser-cooled spectrum, which resolves the hyperfine splittings. We should also verify the known resonance frequency of the $2s\ ^2S \rightarrow 2p\ ^2P$ transition of the $^9\text{Be}^+$ ion, which is an extrapolated value from a measurement at a high magnetic field in a Penning trap [11].

A spectrum of laser-cooled $^9\text{Be}^+$ ions obtained with σ^- radiation is shown in Fig. 3. In this measurement, the number of ions, trapping condition, laser power, and scanning speed were carefully chosen to obtain a near-Lorentzian-shaped spectrum. We also compared this measurement with many different spectra, which often have the typical phase-transition profile [4]. The sharp drops just above the resonance center in these typical spectra were in good agreement

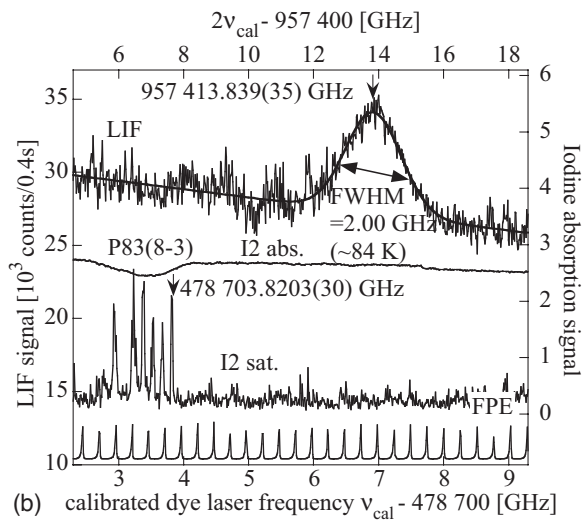
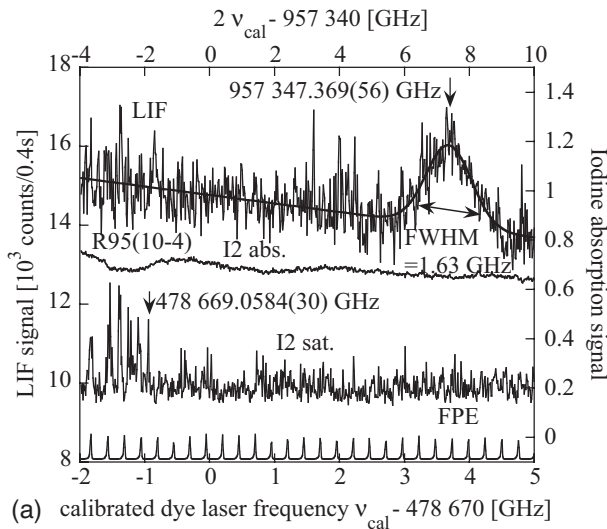


FIG. 2. Laser-induced fluorescence spectra of buffer gas-cooled $^7\text{Be}^+$ (top) and $^{10}\text{Be}^+$ (bottom) ions. Fluorescence intensities as well as absorption signals for frequency markers are recorded as a function of the laser frequency. Doppler-limited absorption signals in the iodine molecule ($\text{I}_2\text{abs.}$), Doppler-free saturation absorption signals ($\text{I}_2\text{sat.}$), and interference fringes of a Fabry-Pérot étalon (FPE) are used for absolute laser-frequency markers. The fundamental IR laser frequencies are indicated at the bottom and the frequency-doubled UV laser frequencies are indicated at the top.

with the resonance center of the spectrum in Fig. 3. We determined the resonant frequency of the $2s\ ^2S_{1/2}; F=2, M_F=-2 \rightarrow 2p\ ^2P_{3/2}; F=3, M_F=-3$ transition of $^9\text{Be}^+$ at $B=0.54$ mT to be

$$\nu_{\text{pump}} = 957\,396.977(14)\ \text{GHz}.$$

With this value the frequency of the transition between the centers of gravity at zero magnetic field ν^9 can be obtained by taking the contributions due to the hyperfine splitting and Zeeman shifts into account as

$$\nu^9 = \nu_{\text{pump}} + (3/4)A_S + \mu_B B = 957\,396.515(14)\ \text{GHz},$$

where $A_S = -625$ MHz is the magnetic hyperfine constant of the ground state of the $^9\text{Be}^+$ ion [5,12] and μ_B is the Bohr

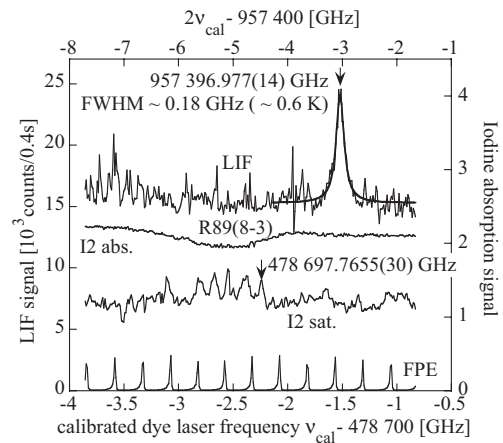


FIG. 3. Laser-induced fluorescence spectrum of laser-cooled $^9\text{Be}^+$ ions.

magneton. The third term is the magnetic-field dependence due to the difference of the g factors in the two states.

Many buffer gas-cooled spectra of $^9\text{Be}^+$ were also measured under similar conditions to the online experiment on $^7\text{Be}^+$ ions, and the results are plotted in a histogram, as shown in Fig. 4. It can be seen that the location of the peak varies somewhat around the average. However, the average value of $957\,396.538(93)$ GHz is in good agreement with ν^9 . From these analyses, we conclude that the peak frequencies measured in the buffer gas-cooled spectra correspond to the transitions between the centers of gravity of the hyperfine splittings within the experimental error. Therefore, we take $\nu^7 = \nu_{\text{gc}}^7$ and $\nu^{10} = \nu_{\text{gc}}^{10}$. However, the width of the fluctuation in these analyses should be added to the systematic error in ν^7 while it is not necessary for ν^{10} , since there are no hyperfine splittings in $^{10}\text{Be}^+$.

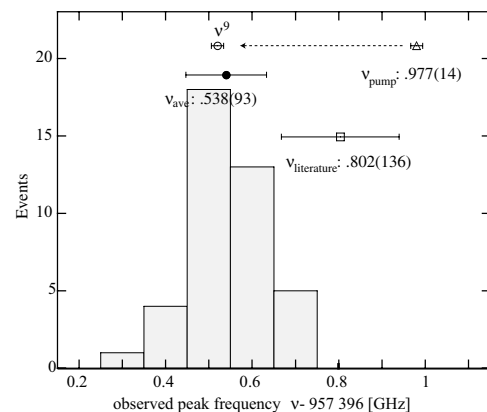


FIG. 4. Histogram of observed peak frequencies of buffer gas-cooled $^9\text{Be}^+$ ions. The average value [\bullet , $957\,396.538(93)$ GHz] is in agreement with the obtained value of the $2s\ ^2S_{1/2} \rightarrow 2p\ ^2P_{3/2}$ transition [\circ , $957\,396.515(14)$ GHz] from the optically pumped $2s\ ^2S_{1/2}; F=2, M_F=-2 \rightarrow 2p\ ^2P_{3/2}; F=3, M_F=-3$ transition frequency (Δ , ν_{pump}) of laser-cooled $^9\text{Be}^+$ ions. The $2s\ ^2S_{1/2} \rightarrow 2p\ ^2P_{3/2}$ transition frequency in Ref. [11] (\square) is also indicated for comparison.

TABLE I. Experimental results for the $2s^2S_{1/2}-2p^2P_{3/2}$ transition of $^{7,9,10}\text{Be}^+$ ($\nu^{7,9,10}$) and results of the fit with Eq. (1) ($\nu^\infty, \kappa/h$). All the frequencies are in units of THz.

A	μ/M_n [10^{-5}] ^a	ν
7	7.819 781 82(13)	957.347 369(124)
9	6.088 204 76(29)	957.396 515(14)
10	5.479 285 28(24)	957.413 839(35)
11	4.978 033 7(31)	957.428 07(36) ^b
∞	0	957.569 55(28)
κ/h		-1884.5(46)

^aAtomic masses M are taken from Ref. [13] and $M_n = M - 4m_e$.

^bEvaluated from the fit values ν^∞ , κ , and the mass of ^{11}Be .

III. DISCUSSION

The final results of the resonance frequencies of the $2s^2S_{1/2}-2p^2P_{3/2}$ transition $\nu^{7,9,10}$ of the $^{7,9,10}\text{Be}^+$ isotope ions and the values of ν^∞ and κ obtained by fitting with Eq. (1) are tabulated in Table I. To clarify the different contributions to the isotope shifts, ν^A is plotted as a function of μ/M_n (Fig. 5). The deviations of each resonant frequency from the fit are indicated in the bottom of Fig. 5. The open box at $A=9$ is an old value from the literature [11]. This large discrepancy from the fit supports our assumption that the extrapolation from the high magnetic field caused a systematic error.

The present experimental results are compared with three different theoretical calculations [14–17], as shown in Table II. Since all the theoretical values are calculated for the energy levels of $2s^2S$ and $2p^2P$ states, ν^∞ for the $2s^2S \rightarrow 2p^2P$ transition is evaluated to be 957 503.83(28) GHz using the fine-structure splitting of 197.150(64) GHz [11] while the dependence of K on the total spin J is ignored. Chung *et al.* [14,15] used a full-core plus correlation (FCPC) method with multiconfiguration interaction (CI) wave functions for the 2^2S state and a restricted variation method (RVM) for the 2^2P state including a relativistic correction. Yan *et al.* [16] used high-precision variational wave func-

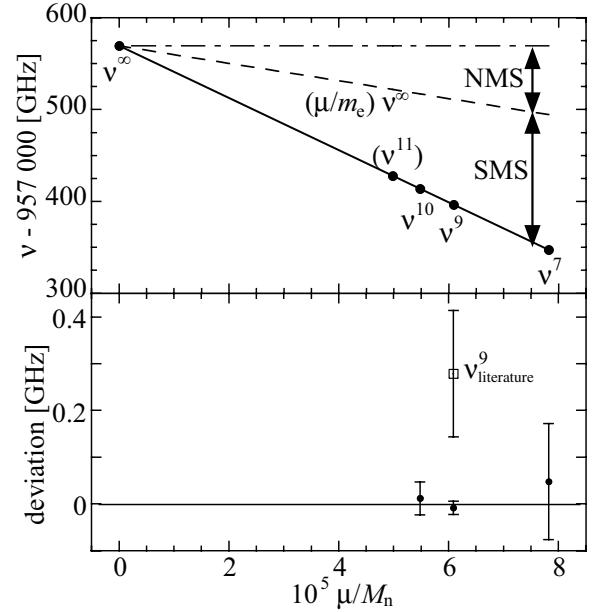


FIG. 5. Resonance frequencies ν^A ($2s^2S_{1/2}-2p^2P_{3/2}$) are plotted as a function of μ/M_n to indicate the two contributions—the NMS and the SMS—to the isotope shifts. The deviations from the fits are also indicated at the bottom.

tions in Hylleraas coordinates. Yamanaka [17] used a configuration interaction (CI) wave function with Slater-type orbitals (STO). For $h\nu^\infty$, the FCPC and RVM methods with relativistic correction give the best value, but it is still smaller than the experimental value by six σ . Other nonrelativistic calculations disagree with the experimental value by more than 0.06%; this is much larger than the quoted uncertainties or displayed digits. It should be noted that the $h\nu^\infty$ values in the FCPC and RVM methods without relativistic correction are almost identical to the value of the Hylleraas calculation. For the differential mass-polarization parameter κ , on the other hand, the Hylleraas calculation agrees within the present experimental uncertainty. In summary, the present theoretical calculations are not sufficient for one of our future goals, namely, to subtract the mass shifts from

TABLE II. Comparisons of the present experimental values of ν^∞ and κ with theoretical values [14–17]. All the values are indicated in units of a.u. $2R_\infty c = 2 \times 3.289\,841\,960\,360(22) \times 10^{15}$ Hz [18] is used in the conversion.

	This work experiment	FCPC (2^2S), RVM (2^2P) [14,15]	Hylleraas [16]	CI (STO) [17]
$\epsilon^\infty(2^2P)$		-14.181 555 7	-14.179 333 3	-14.177 923 8
$\epsilon^\infty(2^2S)$		-14.327 086 3(11)	-14.324 763 2	-14.323 685 7
$h\nu^\infty$	0.145 524 290(42)	0.145 530 6(11)	0.145 429 884	0.145 761 9
$h\nu_{\text{expt}}^\infty - h\nu_{\text{theor}}^\infty$		$-6.3(11) \times 10^{-6}$	$94.41(4) \times 10^{-6}$	-237.6×10^{-6}
$K(2^2P)$		0.166 9	0.165 94	0.165 99
$K(2^2S)$		0.453 4	0.452 70	0.451 25
κ	-0.286 41(70)	-0.287 5	-0.286 76	-0.285 26
$\kappa_{\text{expt}} - \kappa_{\text{theor}}$		$1.1(7) \times 10^{-3}$	$0.35(70) \times 10^{-3}$	$-1.15(70) \times 10^{-3}$

more precise experimental values to deduce the field shift. However, it should be noted that Yang *et al.* [19] have calculated the isotope shifts with much higher accuracies for the neighboring Li atom with the Hylleraas method. The calculation includes relativistic, QED, and other corrections.

IV. CONCLUSION

An online ion trap that is coupled with the projectile fragment separator has been developed at the RIKEN accelerator facility. Energetic, ≈ 1 GeV, radioactive beryllium isotopes from the separator are decelerated, cooled, and finally trapped in a linear rf trap for laser spectroscopy. The atomic transition energies between the ground state and an excited state of the beryllium isotope ions were determined with accuracies of 10^{-8} by straightforward laser-induced fluorescence spectroscopy for buffer gas-cooled ions in the trap. As a result, the transition energy for infinitely heavy mass beryllium ions and the differential mass polarization parameter were determined for the first time. These results allow us to set the laser frequency exactly at the resonance to perform laser-cooling experiments for short-lived beryllium isotopes such as ^{11}Be .

We plan to proceed to isotope shift measurements of even higher accuracies such as 10^{-10} by utilizing the laser-laser double-resonance spectroscopy method [11,20] and frequency comb [21] clockwork frequency calibration in a weak magnetic field. This will enable us to determine the root-mean-square charge radii of the beryllium isotopes when more accurate theoretical atomic structure calculations are provided.

A combination of the charge radii values with the isotope shift measurements and the magnetization distribution with the hyperfine anomaly measurements would allow us to perform complete measurements for the different distributions of neutrons and protons in a nucleus of the beryllium isotopes with a purely electromagnetic probe.

ACKNOWLEDGMENTS

The authors acknowledge the opportunity to use the RIKEN accelerator facility and their work and efforts for providing the radioactive beams. This work was financially supported in part by Grant-in-Aids for Scientific Research on General Area (Grant No. 14340085) from the Japan Society for the Promotion of Science and by the Robert A. Welch Foundation under Grant No. A1546.

-
- [1] M. Wada, Y. Ishida, T. Nakamura, Y. Yamazaki, T. Kambara, H. Ohyama, Y. Kanai, T. M. Kojima, Y. Nakai, N. Ohshima, A. Yoshida, T. Kubo, Y. Matsuo, Y. Fukuyama, K. Okada, T. Sonoda, S. Ohtani, K. Noda, and H. Kawakami, I. Katayama, Nucl. Instrum. Methods Phys. Res. B **204**, 570 (2003).
- [2] M. Wada, Nucl. Instrum. Methods Phys. Res. A **532**, 40 (2004).
- [3] A. Takamine, M. Wada, Y. Ishida, T. Nakamura, K. Okada, Y. Yamazaki, T. Kambara, Y. Kanai, T. M. Kojima, Y. Nakai, N. Ohshima, A. Yoshida, T. Kubo, S. Ohtani, K. Noda, I. Katayama, P. Hostain, V. Varentsov, and H. Wollnik, Rev. Sci. Instrum. **76**, 103503 (2005).
- [4] K. Okada, M. Wada, T. Nakamura, R. Iida, S. Ohtani, J. Tanaka, H. Kawakami, and I. Katayama, J. Phys. Soc. Jpn. **67**, 3073 (1998).
- [5] T. Nakamura, M. Wada, K. Okada, I. Katayama, S. Ohtani, and H. A. Schussler, Opt. Commun. **205**, 329 (2002).
- [6] I. Tanihata, T. Kobayashi, O. Yamakawa, S. Shimoura, K. Ekuni, K. Sugimoto, N. Takahashi, T. Shimoda, and H. Sato, Phys. Lett. B **206**, 592 (1988).
- [7] T. Kubo, M. Ishihara, N. Inabe, H. Kumagai, I. Tanihata, K. Yoshida, T. Nakamura, H. Okuno, and S. Shimoura, Nucl. Instrum. Methods Phys. Res. B **70**, 309 (1992).
- [8] H. Xu, M. Wada, J. Tanaka, H. Kawakami, I. Katayama, and S. Ohtani, Nucl. Instrum. Methods Phys. Res. A **333**, 274 (1993).
- [9] S. Fujitaka, M. Wada, H. Wang, J. Tanaka, H. Kawakami, I. Katayama, K. Ogino, H. Katsuragawa, T. Nakamura, K. Okada, and S. Ohtani, Nucl. Instrum. Methods Phys. Res. B **126**, 386 (1997).
- [10] H. Kato *et al.*, *Doppler-Free High Resolution Spectral Atlas of Iodine Molecule* 15000 to 19000 cm^{-1} (Japan Society for the Promotion of Science, Tokyo, 2000).
- [11] J. J. Bollinger, J. S. Wells, D. J. Wineland, and W. M. Itano, Phys. Rev. A **31**, 2711 (1985).
- [12] D. Wineland, W. M. Itano, and R. S. Van Dyck, Jr., Adv. At. Mol. Phys. **19**, 135 (1983).
- [13] A. H. Wapstra, G. Audi, and C. Thibault, Nucl. Phys. A **729**, 129 (2003).
- [14] K. T. Chung, Phys. Rev. A **44**, 5421 (1991).
- [15] K. T. Chung and X. W. Zhu, Phys. Scr. **48**, 292 (1993).
- [16] Z.-C. Yan, M. Tambasco, and G. W. F. Drake, Phys. Rev. A **57**, 1652 (1998).
- [17] N. Yamanaka, Phys. Lett. A **243**, 132 (1998).
- [18] P. J. Mohr and B. N. Taylor, Rev. Mod. Phys. **77**, 1 (2005).
- [19] Z.-C. Yan and G. W. F. Drake, Phys. Rev. Lett. **91**, 113004 (2003).
- [20] H. G. Dehmelt, *Advances in Atomic and Molecular Physics* (Academic Press, New York, 1969), Vol. 5, pp. 109–154.
- [21] T. Udem, R. Holzwarth, and T. W. Hänsch, Nature (London) **416**, 233 (2002).